The authors would like to thank the editor and referees for the time and effort invested in providing comments and suggestions regarding the paper. Below, we have listed the reviewer comments and addressed them, and incorporated necessary and suggested revisions into the manuscript. Reviewer comments are presented in plain text while our responses are *italicized*.

Reviewer Comments 1:

 Comments on "Mesospheric gravity waves and their sources at the South Pole"

The paper presents an interesting case study using data form 2003 and 2004 at SPA station. Overall I am happy with the paper, there are a couple of things I would like to see changed or added in to make it a better paper. Once these recommendations have been addressed I am happy for the paper to be published.

Minor comments:

Page 2 line 24: define NJIT

We thank you for pointing out this oversight on our part. NJIT is the New Jersey Institute of Technology, the home institution of several of the authors. We have added a clarification of the acronym into the manuscript.

Page 5 line 5: I am assuming that the 94 events that are mentioned here use the ECMWF+NRLMSISE-00 background atmosphere rather than just the climatological background atmosphere? It needs to be clearer which background atmosphere you are using here.

Thank you for your comment. We have added a clarification that the model runs of the 94 wave events used in our study were all performed using a ECMWF+NRLMSISE00 background atmosphere.

Page 6 line 29: The authors are discussing wind divergences as a source of error for their results and say "while a real vertical wind profile over SPA would be ideal, the inclusion of available meteor radar winds at 95km could resolve this problem". If they have the data already and it can help resolve how much error there could be introduced into their ray tracing then they should use it. I would like to see evidence that they have looked at the meteor winds and how they compare to the model winds around the mesopause region. I'd expect there is radiosonde data from SPA too so they would be able to get wind data for the troposphere and lower stratosphere to compare the model winds with too.

Thank you for your comments. While the use of a vertical wind profile at SPA obtained from meteor radar would be ideal, personal communication with the instrument PI have indicated that such a vertical wind profile for the 2003-2004 period of study is not available, and that only

single point measurements at 95 km are available. While these measurements may still be useful in determining wave parameters, we ultimately decided to continue to use MSIS 90 km winds for determining wave parameters.

Page 7 line 2: It is not clear which of the sources they've identified they are saying in an identified one. This should be explained.

Thanks for the comments. In this case we are referring to baroclinic instability as a previously unidentified source mechanism of small-scale waves. We have added a clarification to the manuscript at this line, changing the sentence from "we have presented a compelling case for a previously unidentified source of small-scale gravity waves in the polar MLT." to "we have presented a compelling case for baroclinic instability as a previously unidentified source of small-scale gravity waves observed in the polar MLT."

Figure 1: I find it very difficult to identify the wave fronts in this figure (Figure 2 is better). Maybe you could highlight the wave fronts rather than put and arrow in to make it easier for the reader to identify them?

Thank you for your comments. We have replotted the figures with circles around the waves to make identifying them easier.

Figures 3 and 4: The yellow lines are hard to make out. I'd suggest changing the yellow to something like red and then changing the red line to blue. Also, I appreciate they are showing the vortex shape but seeing the "line" in Figure 3 and 4a is difficult. Maybe they could have a zoomed in plot too showing the line more clearly?

Thank you for the suggestions. We have revised the figures, changing the yellow lines to blue for easier readability. At the present time we feel keeping the "zoomed out" view is better to show the very small deviation from the South Pole of the purely NRLMSISE-00 model runs.

Figure 5: This figure doesn't really convey what the authors say it should, it is quite difficult to make out the contours and the path of the wave just looks like it goes diagonal a bit the straight up. I can't see that this Figure adds anything to the paper so maybe it should be removed. I will leave this decision up to the authors.

Thank you for your comments. The figure is meant to show a 3D projection of the plot shown in Figure 4 (right). It shows the wave ray descending from the observation site above SPA down to the stratosphere, where it bends in the presence of distorted polar vortex wind fields to a termination point which we consider to be the origin of the wave. We have added some clarifying text to the manuscript to make this clearer.

Reviewer's Comments 2:

The paper presents a case study of mesospheric gravity waves detected in airglow emission above the South Pole using data from three austral winter months in 2003 and 2004. The authors identify likely wave source regions based on backward raytraces using the GORGRAT ray-tracing model. Notably, Mehta et al. find evidence for gravity wave sources in the lower mesosphere.

While I enjoyed reading the paper, I feel that limitations and uncertainties associated with backward ray-tracing are not satisfactorily discussed. There are two major sources of error which contribute to uncertainties in the computed trajectories: 1.) uncertainties in the initial wave parameters (horizontal wavelength, direction of propagation, observed period) which are derived from airglow observations in this paper, and 2.) uncertainties in the background wind and temperature fields. Depending on the state of the atmosphere, small changes in the direction of propagation or in the horizontal wavelength may cause the wave's ray path to terminate at vastly different locations.

The problem becomes more severe when the polar vortex is displaced and rays propagate though strong shear flows. As Mehta et al. interpret the termination point of their ray paths as potential gravity wave source regions, uncertainties in the backward trajectories may lead to a large volume with potential sources instead of single source regions. This is my major concern with this case study. The authors compare ray paths which result from using different atmospheric background fields (climatologies and ECMWF analyses). I suggest that the authors also investigate the sensitivity of the wave's ray path to variations in the initial wave parameters. It would be helpful if the authors could provide estimates of the accuracy of their derived wave parameters. For example, Figure 1 looks rather noisy and I find it difficult to motivate a propagation direction of precisely 207_ (page 3, line 20). The same concerns apply to the derivation of the horizontal wavelength and observed period. I recommend the paper for publication provided the issues mentioned above are adequately addressed.

Thank you for your feedback. The reporting of uncertainties and potential sources of error is a major concern and consideration. As pointed out in a later response to Reviewer 3, we have revised our manuscript to include uncertainties on our wave parameter measurements obtained from the image data. We have also performed several model runs using different values within these ranges. Looking at the statistics of this sample of model runs shows a standard deviation of the longitude, latitude, and altitude of the wave ray termination point to be 4.4^o, 2.6^o, and 1.6 km respectively. We have added this error analysis to the manuscript.

Minor comments:

Page 2, line 24: What is NJIT? Please spell out.

We thank you for pointing out this oversight on our part. NJIT is the New Jersey Institute of Technology, the home institution of several of the authors. We have added a clarification of the acronym into the manuscript.

Page 4, line 24: The authors use ECMWF data below 50 km altitude and NRLMSISE-00 an HWM-93 above. How were the data sets stitched together? I assume there are significant differences between a climatological model and ECMWF analyses. The two data sets need to be joined somehow in order to obtain smooth background fields suitable for ray-tracing. I suggest the authors investigate how this "transition zone" affects the computed ray paths (e.g. transition at different altitudes).

Thank you for your comments. The ray-tracing model uses a cubic spline fit from the atmospheric parameters provided by both ECMWF and NRLMSISE-00 in order to construct a smoothed background atmosphere without sharp wind shears and gradients potentially arising from the boundary between the two atmospheric models. We have revised our manuscript to indicate this clearly.

Page 5, lines 2-5: "The polar vortex is displayed away from its normal configuration centered close to SPA and tilted in the region where the wave is determined to originate. This can be seen more clearly in the 3-dimensional projection shown in Figure 5." The contour lines are difficult to relate to the coordinate system in the 3D projection. I suggest a 2D plot like Figure 4.

Thank you for your suggestions. Figure 5 is a 3-dimensional plot of Figure 4, so replacing it with a 2D plot would be redundant. We have amended lines 2-5 to read "The polar vortex is displaced away from its normal configuration centered close to SPA and tilted in the region where the wave is determined to originate. This can be seen more clearly in the 3-dimensional projection shown in Figure 5, which is a projection of the 2D plot shown in Figure 4 (right)."

Figure 5: The kink in the wave's ray path at _43 km looks suspicious to me. The authors combine climatological winds with ECMWF analyses. I expect significant differences in the wind fields, especially when the vortex is displaced. This may introduce artificial wind shears and thus refraction of gravity waves where the two data sets are joined.

Thank you for the comments. While the use of two different background atmospheres can introduce artificial wind shears and wave refraction, the appearance of the "kink" at 43 km is not likely due to the interface of the two atmospheres, as this occurs at 50 km.

Page5, lines 5-14: I assume ECMWF data were used as background fields in the lower atmosphere (no "climatological" runs). Please clarify.

Thank you for the comments. This is correct, and we have added clarification to the manuscript.

Page 6, line 28: "Low" winds at the pole during winter may help to reduce the error in estimates of intrinsic wave parameters, but even small wind speeds can cause gravity waves to be significantly refracted if the waves encounter strong shear flows. This may happen when the vortex is displaced.

Thank you for your comments. While this is true, the line was meant more as a general statement on expected error in the presence of winds diverging from empirical model data, and was not meant to suggest that no errors were expected to arise from the discrepancy between real and empirical winds.

Page 6, line 29: The authors mention that meteor radar winds are available at South Pole. I suggest that the authors use these data instead of the HWM-93 climatology as background winds for ray tracing or at least compare the climatology to observations (meteor radar data) in order to estimate potential errors in ray tracing.

Thank you for your comments. While the use of a vertical wind profile at SPA obtained from meteor radar would be ideal, personal communication with the instrument PI have indicated that such a vertical wind profile for the 2003-2004 period of study is not available, and that only single point measurements at 95 km are available. While these measurements may still be useful in determining wave parameters, we ultimately decided to continue to use MSIS 90 km winds for determining wave parameters. We have revised the manuscript to reflect this.

Page 7, line 2: It is not clear to me what the authors mean by "we have presented a compelling case for a previously unidentified source of small-scale gravity waves in the polar MLT". The backward ray traces presented in this paper terminate at different altitudes in the troposphere, stratosphere and lower mesosphere.

Thank you for your response. We have amended the sentence to read "we have presented a compelling case for baroclinic instability as a previously unidentified source of small-scale gravity waves observed in the polar MLT." in order to clear up that we are referring to the initial observations of the waves in the MLT, which are generated by a previously unidentified lower altitude source, in this case, baroclinic instabilities.

Reviewer Comments 3:

Review opinion on "Mesospheric gravity waves and their sources at the South Pole" by Mehta et al.

Summary:

The manuscript presents interesting analyses on the wave sources of the small-scale gravity waves observed in the winter mesosphere over South Pole. This topic is of great interest to the field of middle atmosphere research since very few studies previously focused on the generation mechanisms of such waves at Polar Regions. Utilizing GROGRAT ray-tracing model and by constructing a background atmosphere with both empirical and more "realistic" model runs, the authors located the sources for 87 wave cases observed by an all-sky imager. The results show that a remarkable number of waves (30 out of 87) are generated near the polar vortex either through baroclinic instability or interactions with planetary waves. The idea that the small-scale gravity waves (<100 km) were generated by baroclinic instability is novel yet needs more evidence and elaborated analyses. I do have a number of major comments that I would like to see the authors address before recommendation for publication.

Major comments:

1. The title does not accurately represent the research in the way that it suggests the scope of the study covers the entire wide spectrum of gravity waves that are observed in the mesosphere over South Pole. But in fact, this study is only focused on the short-period (<14 min) portion of the gravity waves. Add "short-period" in the title.

Thank you for your suggestion, we have amended the manuscript title.

2. In the abstract, the authors mentioned "long vertical wavelength", but then there is no mentioning of vertical wavelength of these short-period gravity waves in the entire main body of the manuscript.

Thank you for your comment. We have removed mention of long vertical wavelength from the abstract.

3. Page1, Line 19: "…, where few manned station exist to operate gravity wave instrumentation during austral winter." Some references to recent mesospheric gravity wave studies at manned station in Antarctica during winter are completely missed. These include [*Chu et al.*, 2011; *Chen et al.*, 2013, 2016; *Kaifler et al.*, 2015] for observations of mesospheric gravity waves during the austral winter in the Antarctic.

Thank you for your comments. It was not our intention to discount the work of other studies in the Antarctic region, but to point out that this work on determining gravity wave sources had

not been achieved, in particular at the polar latitudes. We have added in several of the suggested references, though we have already made several references to Suzuki 2011.

4. Page 3, Line 21: Given the sampling rate is 100 sec (~ 1.7 min), is it really possible to derive wave periods as precise as 0.1 min, as in 7.9 min? Please provide the uncertainty of the derived periods and horizontal wavelengths and a rough estimation of how much the following ray-tracing results may be affected.

Thank you for your comments and concerns regarding error estimation. We have revised our manuscript to include estimates of the measurement error of the wave parameters for the waves in Figures 1 and 2, and discussed the variability in model results arising from these uncertainties. Typical measurement error falls within ± 1 km, ± 1 min, and ± 6°. The measured period should be reported as 8 min ± 1 min.

5. There is meteor radar at South Pole, which provided real horizontal wind data in [*Suzuki et al.*, 2011]. What is the reason for not using the same data set for a realistic background atmosphere? Due to the critical role of a realistic atmosphere background wind play in the ray tracing, at least, it is worthwhile to validate HWM-93 with the meteor radar observation. If there were a large discrepancy between HWM-93 and the meteor radar winds, how will authors address the effect of such unrealistic atmosphere background on ray tracing. Furthermore, there must be inconsistency between HWM-93 and ECMWF at the transition region (50 km). How did the authors treat this inconsistency?

Thank you for your comments. While the use of a vertical wind profile at SPA obtained from meteor radar would be ideal, personal communication with the instrument PI have indicated that such a vertical wind profile for the 2003-2004 period of study is not available, and that only single point measurements at 95 km are available. While these measurements may still be useful in determining wave parameters, we ultimately decided to continue to use MSIS 90 km winds for determining wave parameters.

6. The identifications of baroclinic instability in Figure 7 and signature of planetary waves in Figure 8 are not clear and hard to follow in both the text and figures. Please elaborate your analysis on the part how the baroclinic instability is inferred from 24-hour differenced geopotential maps. It is also helpful to mark the related features on Figures 7 and 8.

Thank you for your comments. We have marked the regions where we have inferred baroclinic instability with a yellow oval in the plots, and have included clarification in the figure caption.

Clarifications and technical issues

1. Page 5, Line 12: "Of the 30 remaining waves, half were traced…, and the other half"

Thank you, we have fixed this typo in the manuscript.

2. Page 5, Line 27: should be "analyses".

Thank you, we have fixed this typo in the manuscript.

Figures:

1. The red 'X' in Figures 7 and 8 are too small to find.

Thank you for your feedback, we have enlarged the red 'X's as well as marking the regions where we are inferring the formation of baroclinic instabilities with a yellow oval

References
Chen, C., X. Chu, A. J. McDonald, S. L. Vadas, Z. Yu, W. Fong, and X. Lu (2013), Inertia-gravity waves in Antarctica: A case study using simultaneous lidar and radar measurements at McMurdo/Scott Base (77.8°S, 166.7°E), *J. Geophys. Res. Atmos.*, *118*(7), 2794–2808, doi:10.1002/jgrd.50318.
Chen, C., X. Chu, J. Zhao, B. R. Roberts, Z. Yu, W. Fong, X. Lu, and J. A. Smith (2016), Lidar observations of persistent gravity waves with periods of 3-10 h in the Antarctic middle and upper atmosphere at McMurdo (77.83°S, 166.67°E), *J. Geophys. Res. Sp. Phys.*, *121*(2), 1483–1502, doi:10.1002/2015JA022127.
Chu, X., Z. Yu, C. S. Gardner, C. Chen, and W. Fong (2011), Lidar observations of neutral Fe layers and fast gravity waves in the thermosphere (110-155 km) at McMurdo (77.8°S, 166.7°E), Antarctica, *Geophys. Res. Lett.*, *38*(23), L23807, doi:10.1029/2011GL050016.
Kaifler, B., F.-J. Lübken, J. Höffner, R. J. Morris, and T. P. Viehl (2015), Lidar observations of gravity wave activity in the middle atmosphere over Davis (69°S, 78°E), Antarctica, *J. Geophys. Res. Atmos.*, *120*(10), 4506–4521, doi:10.1002/2014JD022879.
Suzuki, S., M. Tsutsumi, S. E. Palo, Y. Ebihara, M. Taguchi, and M. Ejiri (2011), Shortperiod gravity waves and ripples in the South Pole mesosphere, *J. Geophys. Res.*, *116*(D19), D19109, doi:10.1029/2011JD015882.

Changes in the manuscript:

Title revised to "Short-period mesospheric gravity waves and their sources at the South Pole"

Revised the abstract to omit references to "long vertical wavelengths"

Page 1, line 19: added references suggested by Reviewer 3.

Page 2, line 27: added clarification of the acronym "NJIT"

Page 3, line 24 and 26: added uncertainties to the measured gravity wave parameters.

Page 4, line 28-30: added clarification on the cubic spline fit used in constructing the background atmosphere, in order to smooth out any potential artificial wind shears at the boundary between the ECMWF and NRLMSISE-00 regimes.

Page 5, line 7-9: Amended the lines to read "The polar vortex is displaced away from its normal configuration centered close to SPA and tilted in the region where the wave is determined to originate. This can be seen more clearly in the 3-dimensional projection shown in Figure 5, which is a projection of the 2D plot shown in Figure 4 (right)." in order to clear up confusion regarding Figure 5

Page 5, line 9-10: added discussion of variability in the model results arising from uncertainties in the measurement of gravity wave parameters from the image data.

Page 5, line 11-12: added clarification that the model runs for the 94 wave events were performed using a background atmosphere constructed from NRLMSISE-00 above 50 km and ECMWF reanalyses below 50 km.

Page 7, line 9-10: revised the line to read "we have presented a compelling case for baroclinic instability as a previously unidentified source of small-scale gravity waves observed in the polar MLT." providing clarification that we are referring to waves observed in the MLT and that baroclinic instability is the previously unidentified source of these small-scale waves.

Figure 1:

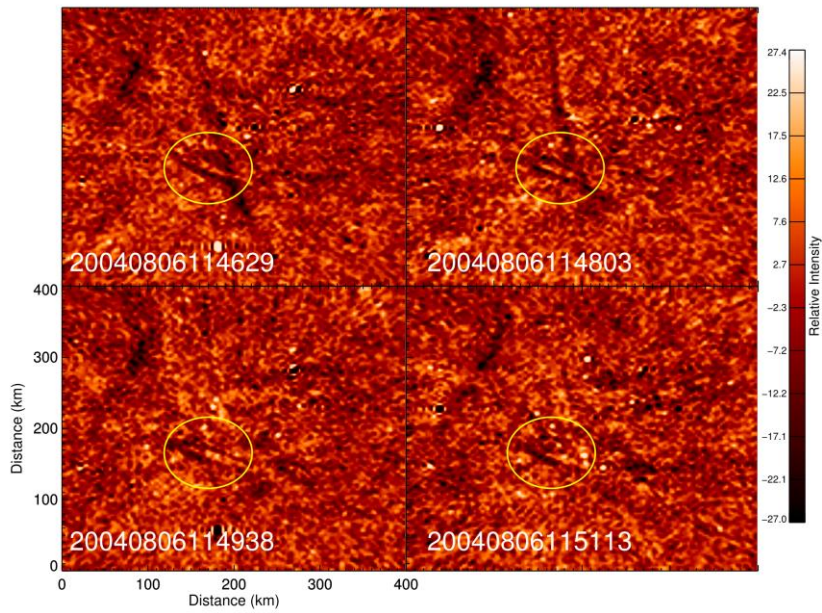We have added yellow circles to better show the waves in the images, as seen below.

Figure 2:

We have similarly added yellow circles to this plot to better show the waves in the images, as seen below.
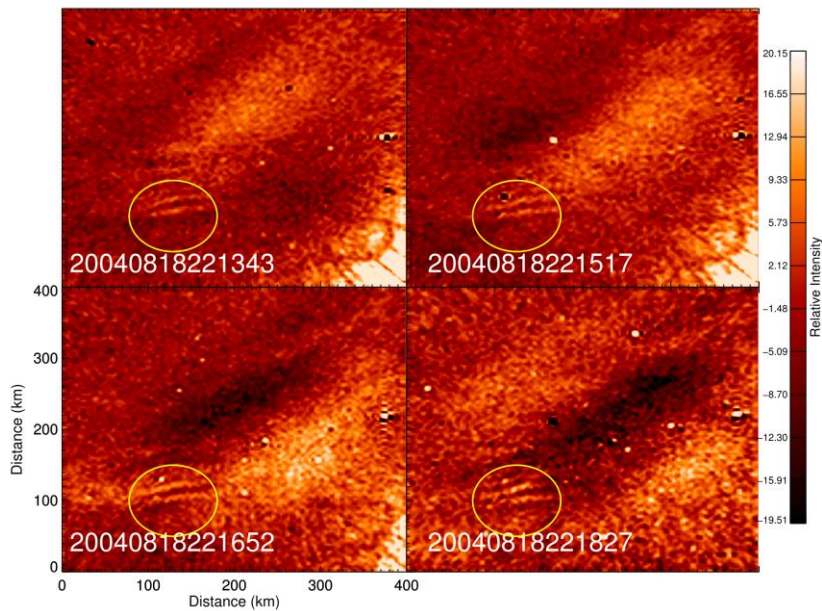

Figure 3:
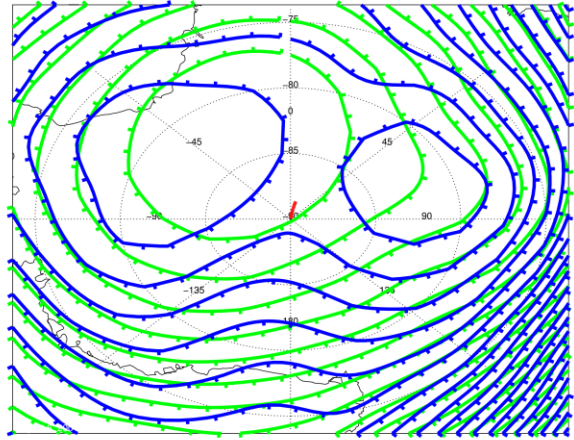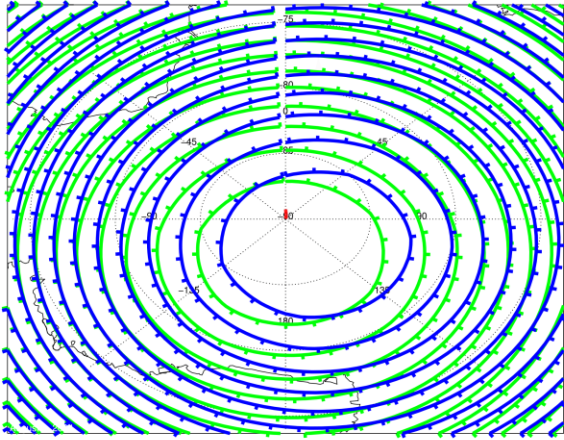Changed the yellow contours to blue for easier readability.
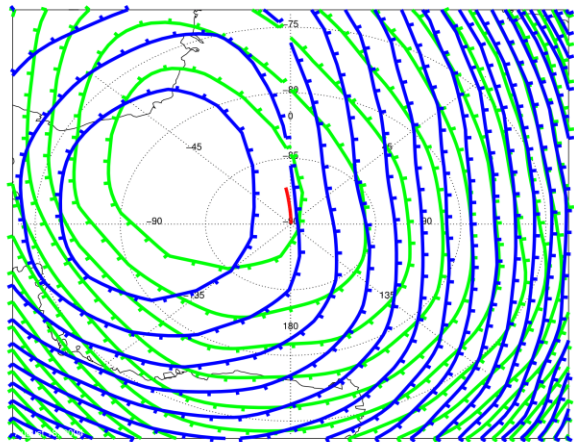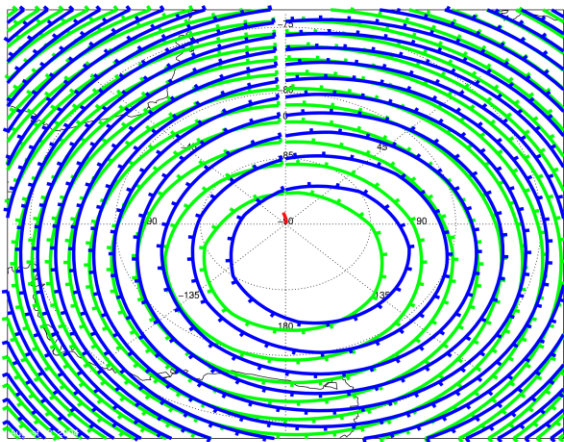
Figure 4:
Same as Figure 3.

Figure 5:
Changed contour colors to match previous to figures.
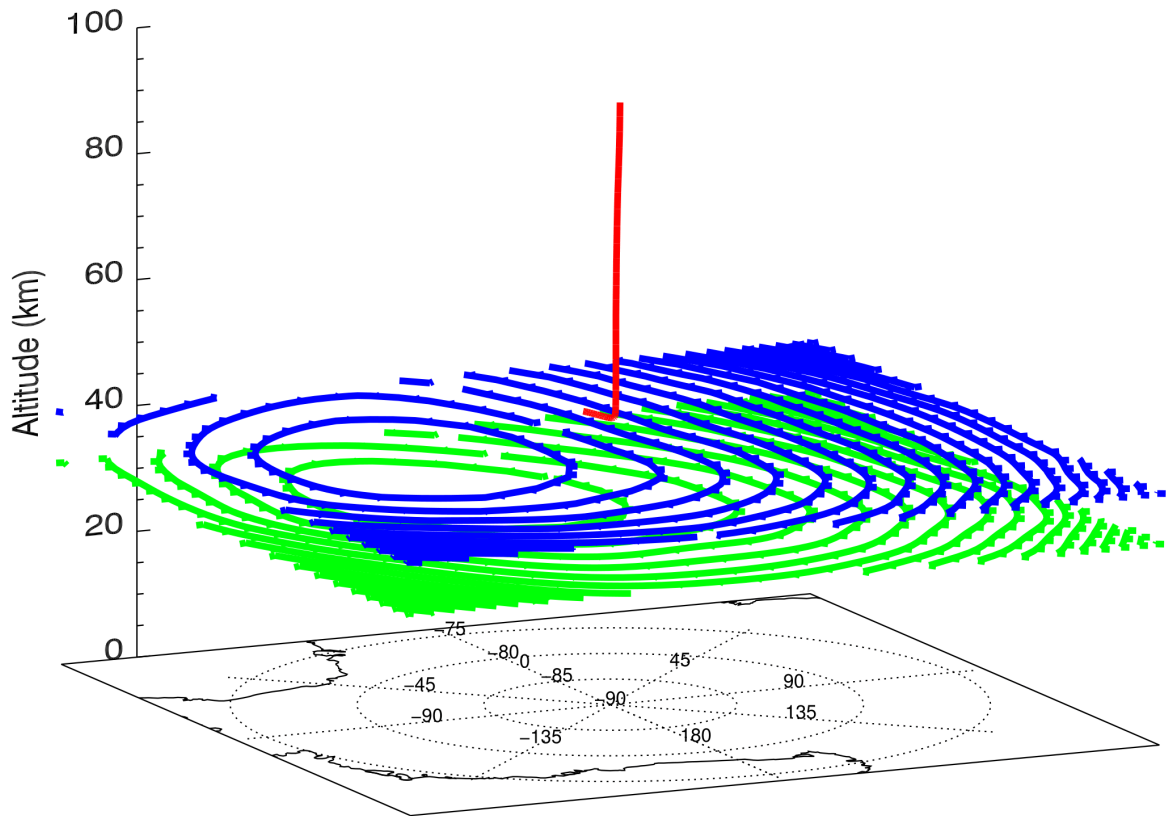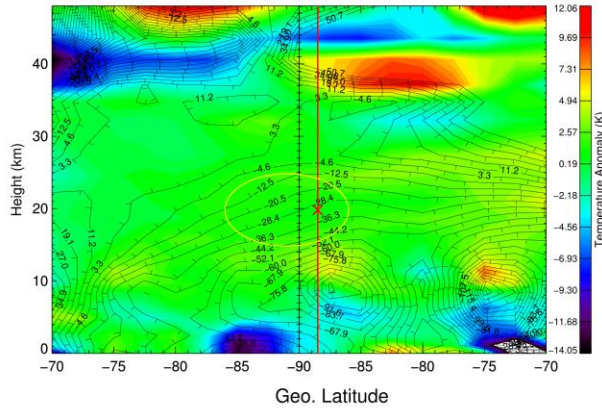
Figure 7:
Added yellow ovals to denote regions where we infer baroclinic instability. Amended the figure caption to reflect this.

July 18, 2003

July 22, 2003

August 2, 2003

August 18, 2004

%% Copernicus Publications Manuscript Preparation Template for LaTeX Submissions

%% 2-Column Papers and Discussion Papers
\documentclass[acp, manuscript]{copernicus}

\begin{document}

\title{Short-period mesospheric gravity waves and their sources at the South Pole}

% \Author[affil]{given_name}{surname}

\Author[1]{Dhvanit}{Mehta}
\Author[1]{Andrew J.}{Gerrard}
\Author[2]{Yusuke}{Ebihara}
\Author[3]{Allan T.}{Weatherwax}
\Author[1]{Louis J.}{Lanzerotti}

\affil[1]{Center for Solar-Terrestrial Research, New Jersey Institute of Technology, 323 Martin Luther King Jr. Boulevard, 101 Tiernan Hall, Newark, NJ 07102-1982, USA.}
\affil[2]{Research Institute for Sustainable Humanosphere, Kyoto University, Gokasho, Uji City, Kyoto Prefecture, Japan.}
\affil[3]{Merrimack College, 315 Turnpike St, North Andover, MA 01845, USA.}

\runningtitle{GRAVITY WAVE SOURCES AT THE SOUTH POLE}

\runningauthor{D. Mehta}

\correspondence{D. Mehta\\ (dm36@njit.edu)}

\received{}
\pubdiscuss{} %% only important for two-stage journals
\revised{}
\accepted{}
\published{}

%% These dates will be inserted by Copernicus Publications during the typesetting process.

\firstpage{1}

\maketitle

\begin{abstract}
The sourcing locations and mechanisms for short period, long vertical wavelength upward-propagating gravity waves at high polar latitudes remain largely unknown. Using all-sky imager data from the Amundsen-Scott South Pole Station we determine the spatial and temporal

characteristics of 94 observed small-scale waves in three austral winter months in 2003 and 2004. These data, together with background atmospheres from synoptic and/or climatological empirical models, are used to model gravity wave propagation from the polar mesosphere to each wave's source using a ray-tracing model. Our results provide a compelling case that a significant proportion of the observed waves are launched in several discrete layers in the tropopause and/or stratosphere. Analyses of synoptic geopotentials and temperatures indicate that wave formation is a result of baroclinic instability processes in the stratosphere and the interaction of planetary waves with the background wind fields in the tropopause. These results are significant for defining the influences of the polar vortex on the production of these small-scale, upward propagating gravity waves at the highest polar latitudes.
\end{abstract}

\introduction

The breaking and induced drag caused by atmospheric gravity waves plays an important role in the dynamics of the mesosphere-lower thermosphere (MLT) region \citep{fritts2003}. The impacts of such wave breaking is felt on a climatological scale; e.g. gravity waves fundamentally drive a meridional circulation resulting in a cool summer mesopause and warm winter mesopause \citep{meriwether2004}. On the synoptic scale the effects of gravity waves can be seen in the localized destruction of mesospheric clouds \citep{gerrard2002synoptic, gerrard2004}, mesospheric fronts/bores \citep{brown2004}, and localized wave ducting \citep{li2011}. As such, because of their significance to the dynamics of the middle atmosphere gravity waves have been a focus of active and ongoing research, particularly at high latitudes. However, while some studies have looked at gravity waves near the poles \citep{chu2011,chen2013,kaifler2015}, observations at high latitudes are often difficult to obtain due to experimental logistics. This is even more of an issue in the Antarctic region, where few manned stations exist to operate gravity wave instrumentation during the austral winter.

Of particular interest to this study is the determination of high latitude gravity wave source regions. Many studies have investigated the excitation of gravity waves in the lower atmosphere \citep{sato2008, gerrard2011, moffat2011}, directly in the MLT region from auroral heating \citep{oyama2012}, and on the characteristics and seasonal variation of gravity waves in the polar MLT region \citep{nielsen2012, suzuki2011}. While the excitation and propagation of gravity waves during disturbed conditions, such as during sudden stratospheric warmings and stratospheric temperature enhancements \citep{meriwether2004}, have been investigated by \citet{wang2009, yamashita2010, gerrard2011}, there is a significant gap in understanding of wave generation during quiet conditions or from a climatological or quasi-climatological perspective.

One dominant gravity wave source region known to occur at polar latitudes is the polar vortex \citep{duck1998, whiteway1999}. Displacement of the polar vortex away from its mean position over a pole can result in a vertically slanted, tilted wind structure that can give rise to baroclinic instabilities \citep{tanaka2002}. These instabilities have been studied as a generating mechanism for larger-scale (on the order of several hundred kilometer) gravity waves through extensive

modeling \citep{fairlie1990, o'sullivan1995, plougonven2007, lin2008} and observational \citep{guest2000, plougonven2003, lane2004, gerrard2011} efforts, but to date their status as a source of small scale gravity waves ($<$ 100 km) has not been investigated.

In this paper we show gravity wave observations from South Pole Station, Antarctica (hereafter SPA) from a dataset previously presented in \citet{suzuki2011}. We then model the propagation of the observed waves from their site of observation above SPA to their lower altitude sources using ray-tracing techniques. We then analyze the potential source regions of the waves using lower atmospheric analyses. In Section 2 we present our gravity wave observations. In Section 3, the results of our ray-tracing model runs are presented, with results showing stratified layers of gravity wave sources in a region around the SPA site tightly restricted in latitude. In Section 4, we show lower atmospheric analyses that support the results of our modeling efforts and our interpretation of baroclinic instability as the primary mechanism of gravity wave generation by the polar vortex. Finally, we present conclusions in Section 5, with a discussion as to the challenges and limitations of our investigation.

\section{Gravity wave observations}

For this study we utilized data obtained from a multi-wavelength all-sky imager located at SPA, originally constructed and operated by the National Institute of Polar Research (NIPR), and now operated by the Research Institute for Sustainable Humanosphere (RISH) of Kyoto University, Japan, in collaboration with the New Jersey Institute of Technology (NJIT) \citep{Ejiri1999, suzuki2011}. The imager consists of a fish-eye lens providing 180$\degree$ field of view (Nikkor \textit{f} = 6 mm, F1.4), a rotating filter wheel with five filters (427.8 nm, 557.7 nm, 630.0 nm, 589.0 nm, 486.1 nm) for both auroral and airglow observations, and a temperature controlled CCD camera with 512 x 512 pixel resolution. Due to its location at SPA, the system is able to operate more or less continuously during the austral winter period, between April and August barring periods where the moon is at high elevation angle. In this paper we chiefly focused on the green line OI (557.7 nm) and Na (589.0 nm) airglow filters. For data shown from 2003 and 2004, Na images have 64 sec exposure times and are taken roughly 100 sec apart, while green line images are taken with 8 sec exposures, also at 100 sec sampling rate.

Gravity wave observations have previously been reported with this instrument using its Na airglow filter for the 2003-2005 austral winters by \citet{suzuki2011}, providing a climatology of waves observed at $\sim$95 km for both larger-scale ``band'' events as well as smaller scale ``ripple'' events that are commonly thought to be localized convective or dynamical instability processes. For our own analysis, we used a portion of this data set covering July 2003, August 2003, and August 2004 as these periods showed the highest continuous Na airglow observations with minimal contamination by auroral emissions. Note that while the 589.3-nm emission is generally not sensitive to auroral contamination, we nonetheless found the presence of auroral emissions in our image data, likely as a result of spectral leakage due to complications with the filter. While this contamination was only problematic during periods where the auroral emissions were particularly bright, its persistence throughout the data set meant we were forced to compare

our images with roughly simultaneous green-line 557.7 nm filter images taken from the same instrument. This allowed us a greater accuracy in differentiating between auroral processes and gravity wave signatures in our Na images and allowed us to observe gravity waves even in conditions where portions of the image were contaminated.

Prior to analyzing images for the signatures of gravity waves, it was necessary to apply a number of post-processing techniques to the data. First, to correct for distortion of the image as a result of the fish-eye lens, images were unwarped using the technique described in \citet{Garcia1997} into geographic coordinates from the original ``warped'' image coordinate frame. Next, the resultant images were time-differenced in order to heighten image contrast and make it possible to identify gravity wave structure in the fairly faint airglow emission. Finally, the images were band pass filtered. While many studies using newer imager systems eschew time-differencing due to the potential introduction of artifacts, it was necessary in our analysis due to the faintness of the emission, as well as the significant difference in contrast between airglow and auroral contamination any time contamination was present. Once the images were fully processed, images were inspected for the presence of gravity waves and their observed horizontal wavelengths, periods, and propagation directions were measured and recorded.

From the 38 days of available data during July 2003, August 2003, and August 2004, we observed 94 total wave events. Examples are shown in Figures \ref{Aug06Wave} and \ref{Aug18Wave}. In Figure \ref{Aug06Wave}, for August 6, 2004, a gravity wave is seen propagating southward at 207 $\pm$ 6$\degree$ with λ_h = 17 $\pm$ 1 km and T_{obs} = 8 $\pm$ 1 min beginning around 11:37 UT and leaving the imager FOV at 12:07 UT (where "North" here is defined as being along 0$\degree$ longitude by convention). Figure \ref{Aug18Wave}, for August 18, 2004, shows a gravity wave propagating south at 157 $\pm$ 6$\degree$ with λ_h = 16 $\pm$ 1 km and T_{obs} = 8 $\pm$ 1 min, first appearing at 21:54 UT and departing from the imager FOV at 22:32 UT.

We then proceeded to perform an initial series of ray-tracing runs using these two waves. Our goal was two-fold: first, as a proof of concept for the application of the ray-tracing model to waves in the polar MLT, and second to demonstrate the need to run the model on an atmospheric background with synoptic-scale variation. Following this, we performed ray-tracing model runs on the remainder of the gravity waves in the dataset.

\section{Gravity wave source determination using the GROGRAT ray-tracing model}

Ray-tracing techniques have been applied for decades in modeling the propagation of waves through the atmosphere \citep{lighthill1978}. \citet{dunkerton1984} used a simple hydrostatic ray tracing scheme to show that meridional asymmetry in the background flow due to a sudden stratospheric warming led to regions through which stationary gravity waves with horizontal wavelengths between 50-200 km could not propagate due to critical level filtering. The development of a full, three dimensional nonhydrostatic (i.e. one in which $\frac{\partial p^\prime}{\partial z} + \rho g \neq 0$) ray tracing algorithm by \citet{marks1995}, and their

subsequent additions in \citet{eckermann1997} led to the Gravity Wave Regional or Global Tracer (GROGRAT) ray tracing model. The model tracks the amplitude evolution and four dimensional propagation of a wave through a background atmosphere and includes terms for radiative dissipation, amplitude saturation, and turbulent diffusion, with an upper altitude limit of 120-km. The model utilizes an internal regridding scheme that permits the use of practically any input background atmosphere, allowing for the incorporation of multiple atmospheric data products into a single run regardless of their original grid.

GROGRAT has been used in a number of studies of wave propagation, both running in reverse for the purpose of determining tropospheric wave sources \citep{gerrard2004, brown2004, Vadas2009}, and for forward modeling \citep{lin2008, yamashita2013} the ray propagation from baroclinic regions or during disturbed conditions, such as during sudden stratospheric warmings. Ray-tracing analysis has previously been applied to the high latitude MLT by \citet{yamashita2013} in their study of gravity wave propagation during sudden stratospheric warming events, albeit with an arbitrary spectrum of waves originating in the troposphere and propagating into the middle atmosphere under varying background conditions. For our analysis of wave sources over SPA, we also utilized GROGRAT v2.9, with a grid displaced 4$\degree$ latitude from SPA. This avoid complications around the pole arising from the singularity at -90$\degree$ latitude. We ran the model on a global 2.5$\degree$ x 2.5$\degree$ spatial grid with 50 altitude levels spaced 2 km apart centered over the SPA site.

An important consideration in applying reverse ray-tracing techniques to gravity wave propagation through the atmosphere is the construction of an accurate atmospheric background through which the wave ray path is integrated. Two options were investigated and are presented in example runs for the waves shown in Figures \ref{Aug06Wave} and \ref{Aug18Wave}. The first is a purely ``climatological'' atmosphere and the second is an atmosphere that incorporates synoptic variation below 50-km. ``Climatological'' runs used a background atmosphere constructed from the Navy Research Laboratory Mass Spectrometer and Incoherent Scatter Radar (NRLMSISE-00) \citep{picone2002} empirical atmospheric model and the Horizontal Wind Model (HWM-93), an empirical horizontal neutral wind model of the upper atmosphere \citep{hedin1996}, for the entire atmosphere from the surface to 120-km altitude. ``Synoptic'' runs utilized the European Centre for Medium-Range Weather Forecasts (ECMWF) Tropical Ocean and Global Atmospere (TOGA) \citep{cisl_rda_ds111.2} 2.5$\degree$ Global Surface and Upper Air Analysis datasets below 50-km, with NRLMSISE-00 and HWM-93 input from 50-km to 100-km, where the background atmospheric parameters were smoothed using a cubic spline fit to prevent artificial wind shears and similar features at the boundary at 50 km. Gravity waves were initiated at 95 km with prescribed spatial and temporal characteristics as determined by our analysis of the all-sky imager data. The results for the wave observed on August 6, 2004 are shown in Figures \ref{040806Runs}a and \ref{040806Runs}b for the climatological and synoptic runs respectively. Those for August 18, 2004 are shown in Figures \ref{040819Runs}a and \ref{040819Runs}b for the climatological and synoptic runs respectively.

For the August 6th wave, both types of runs show gravity wave rays terminating in the troposphere, at 7 km altitude for the climatological run and at the surface for the synoptic run. However, the ray paths for the two model runs differ significantly in both direction of propagation and distance from SPA. During this period, the polar vortex, through which the

wave propagates, is fairly stable as seen in the NRLMSISE-00 background in Figure \ref{040806Runs}a, while the shape of the vortex seen in the ECMWF background in \ref{040806Runs}b is distorted by apparent interaction with a planetary wave.

A different result is seen for the wave observed on August 18. The climatological run once again produces a ray path stopping in the troposphere near SPA at an altitude of 7 km. In the ECMWF-based synoptic model run the ray path travels down into the stratosphere, where it travels farther out than for the climatological run, before stopping at a height of 42.5-km roughly 3.5$\degree$ latitude from SPA. The polar vortex is displaced away from its normal configuration centered close to SPA and tilted in the region where the wave is determined to originate. This can be seen more clearly in the 3-dimensional projection shown in Figure \ref{Aug19Foregrats3d}, which is a projection of the 2D plot shown in Figure 4 (right). Typical uncertainties in the model results arising from uncertainties in the measurement of wave parameters are around 4.4$\degree$ longitude, 2.6$\degree$ latitude, and 1.6 km altitude.

All 94 wave events were ray-traced using GROGRAT, using the background atmospheres constructed from ECMWF reanalyses below 50 km and NRLMSISE-00 above 50 km. Seven waves were found to be evanescent, indicating they are not propagating gravity waves and are likely to be observations of local convective or dynamical instability processes in the mesopause over SPA. Figure \ref{PhaseSpeed} shows plots comparing the source region heights with observed wave parameters for the remaining 87, freely propagating, waves. 41 of the gravity waves were traced to tropospheric sources, while 16 waves originated above 50-km. As ECMWF does not extend beyond 50-km altitude, we were unable to analyze the sources of these waves. As shown in Figure \ref{PhaseSpeed}, there is no correlation between the height of the wave sources and the spatial and temporal characteristics of the waves. Of the 30 remaining waves, 15 were traced into the tropopause between 9 km and 15 km and the other half into the stratosphere between 15 km and 50 km. Based on our results the gravity waves above SPA appear to originate in several discrete layers centered at 65 km, 40 km, the tropopause, and the surface. All but 6 of the waves originated within 2.5$\degree$ latitude of SPA, as seen in the bottom right panel of Figure \ref{PhaseSpeed}, which shows the distrubution of the 87 freely propagating waves around SPA.

\section{Analysis of Background Source Conditions using ECMWF Reanalysis}

In order to identify possible wave generating regions for our the observed waves and modeled wave sources, we examined the background atmospheric conditions around SPA, within the limitations of available data products for the Antarctic lower and middle atmosphere. For this investigation we analyzed 24-hour time-differenced geopotential heights and temperatures obtained from ECMWF Reanalysis from the surface up to 50-km, the upper limit on ECMWF. We mapped 24-hour differenced geopotential heights and temperatures along the wave ray paths as determined by the GROGRAT model runs, as well as in the longitudinal direction opposite from the wave's ray path, such that each slice of data corresponded to a single longitude bin between 0-50 km altitude and -70$\degree$ to -70$\degree$ latitude. By examining 24-hour variations, we are able to see shifts in the structure of the polar vortex towards configurations of

high baroclinicity that we would not otherwise be able to as easily infer from the raw geopotential height and temperature maps. Then, by comparing these differenced maps to the wave ray paths we can determine if wave sources match regions where baroclinic instabilities or other observable wave source regions are likely to occur.

Figure \ref{StratWaves} shows 24-hour time differenced ECMWF geopotential height and temperature analyses of waves that were found to form in the stratosphere from July 18, 2003, July 22, 2003, August 2, 2003, and August 18, 2004, in regions where the differenced geopotential height maps are heavily slanted latitudinally and vertically, indicating a displacement of the polar vortex that has moved the polar vortex ``off-balance'' and has likely set up the baroclinic instability that is driving wave excitation. At mid-latitudes a westward tilt is required for a baroclinic wave to draw potential energy from the westerly mean flow \citep{holton1982}, but at polar latitudes any displacement from the mean configuration centered over pole is seen as a generator of gravity waves. Our analysis is further complicated by the lower number of latitude bins near the pole, particularly when one considers that the majority of observed wave sources come from within 2.5$\degree$ of SPA. While the direction of tilt can vary latitudinally either towards or away from the pole, this does not appear to affect the formation of the waves, though this may affect the direction of horizontal wave propagation, which would become apparent in a more thorough study over an extended period.

Plots for waves observed on July 19, August 3 and August 17, 2003, and August 9, 2004 are shown in Figure \ref{TropoWaves}. These waves form in the tropopause in regions of disturbed geopotentials and temperatures. The signature of a planetary wave is present in each case in the vicinity of the wave source, which is the likely cause of the vertical forcing that is generating the waves over SPA. This structure is found in all 15 cases of waves generated in the tropopause.

\section{Discussions and conclusions}
Our observations and model analyses demonstrate that any displacement of the polar vortex, whether locally in the tropopause due to the planetary wave interaction or as a whole in the stratosphere, is sufficient to generate upward propagating, and thus upward momentum transporting, gravity waves above the troposphere. However, several questions and concerns still remain. We are limited in terms of the available dataset both due to repeated $>$7 day long gaps for which no Na airglow data is available as well as the near constant presence of auroral contamination in the filter for all UT except the early morning. While there are other days available for the 2003-2005 austral winters, as previously analyzed by \citet{suzuki2011}, these are largely disparate and spread out with larger gaps for which no Na data is available, and thus we have ignored these for now, focusing on periods of continuous observation over $\sim$7 day intervals.

Due to the rapidly changing background atmospheric conditions responsible for gravity wave excitation, and our reliance on NRLMSISE-00 and HWM-93 climatologies above 50 km, we are able to analyze the results of the ray tracing runs with ray paths terminating in the mesosphere to

only a limited extent. Two examples of this are runs for August 6th and 7th, 2004, where the wave rays originated at 65 km. Differenced geopotential and temperature plots for these two cases are shown in Figure \ref{MesoWaves}. As the polar vortex extends upward into the MLT, the apparent disturbance of the polar vortex below 50 km seen in both figures should similarly extend upward, and is likely to be the source of the waves we observed over the SPA site. However, without the availability of a model that can account for synoptic-scale variation for the polar mesosphere for this time period we are unable to further our analysis. This is unfortunate, as waves in this region account for 16 of the 87 waves found by our model to be real, propagating waves, and this is roughly equal in number to the waves originating from the stratosphere or tropopause.

Another consideration is our current reliance on model winds for the characterization of gravity wave intrinsic frequencies and vertical wave numbers, both necessary components as inputs into GROGRAT. Any divergence of the real background winds from the model represents a source of error for our model runs, though with winds typically being low near the pole during winter this is not expected to be a large error source. While a real vertical wind profile over SPA would be ideal, the inclusion of available meteor radar winds at 95 km could resolve this problem, however at the present time we have elected not to include this data, as we are unable to adequately constrain the winds with a single point measurement at 95 km.

In this paper, we have shown through the combination of observation and numerical modeling that the polar tropopause and stratosphere is a frequent source of upward propagating gravity waves. While there are inherent limitations to our analysis both in terms of available image and atmospheric data and in refining our modeling efforts with additional, existing data, we have presented a compelling case for baroclinic instability as a previously unidentified source of small-scale gravity waves observed in the polar MLT..

Previous analyses of the Arctic polar vortex by \citet{bhattacharya2010} have looked at the response of the polar vortex during quiet conditions to drivers in the MLT as a form of downward control by thermospheric winds. These winds are known to, in turn, respond to variations in gravity wave input into the region. With both upward and downward energy transport affecting dynamics throughout the lower and middle atmosphere, we are left with an extensive coupled system with built-in feedback mechanisms. The excitation of gravity waves in the tropopause and stratosphere by the establishment of baroclinic instabilities through displacement of the polar vortex is an important component in the system in need of further study.

%% REFERENCES
\begin{thebibliography}{}

\bibitem[{Bhattacharya and Gerrard(2010)}]{bhattacharya2010}
Bhattacharya, Y. and Gerrard, A.: Correlations of mesospheric winds with subtle
motion of the Arctic polar vortex, Atmos. Chem. Phys., 10,
431--436, 2010.

\bibitem[{Brown et~al.(2004)Brown, Gerrard, Meriwether, and Makela}]{brown2004}
Brown, L., Gerrard, A., Meriwether, J., and Makela, J.: All-sky imaging
observations of mesospheric fronts in {OI} 557.7 nm and broadband {OH} airglow
emissions: Analysis of frontal structure, atmospheric background conditions,
and potential sourcing mechanisms, J. Geophys. Res., 109, 2004.

\bibitem[{Chen et~al.(2013)Chen, Chu, McDonald, Vadas, Yu, Fong, and Lu}]{chen2013}
Chen, C., Chu, X. McDonald, A.~J., Vadas, S.~L., Yu, Z., Fong, W., and Lu, X.: Inertia-gravity
waves in
Antarctica: A case study using simultaneous lidar and radar measurements at McMurdo/Scott
Base
(77.8$\degree$S, 166.7$\degree$E), J. Geophys. Res., 118(7), 2794-2808,
doi:10.1002/jgrd.50318.

\bibitem[{Chu et~al.(2011)Chu, Yu, Gardner, Chen, Fong}]{chu2011}
Chu, X., Yu, Z., Gardner, C.~S., Chen, C., Fong, W.: Lidar observations of neutral Fe layers and
fast gravity waves in the thermosphere (110–155 km) at McMurdo (77.8$\degree$S,
166.7$\degree$E),
Antarctica, Geophys. Res. Lett., 38(23), doi:10.1029/2011GL050016.

\bibitem[{Duck et~al.(1998)Duck, Whiteway, and Carswell}]{duck1998}
Duck, T.~J., Whiteway, J.~A., and Carswell, A.~I.: Lidar observations of
gravity wave activity and {Arctic} stratospheric vortex core warming,
Geophys. Res. Lett., 25, 2813--2816, 1998.

\bibitem[{Dunkerton and Butchart(1984)}]{dunkerton1984}
Dunkerton, T.~J. and Butchart, N.: Propagation and selective transmission of

internal gravity waves in a sudden warming, J. Atmos. Sci., 41, 1443--1460, 1984.

\bibitem[{Eckermann and Marks(1997)}]{eckermann1997}
Eckermann, S.~D. and Marks, C.~J.: {GROGRAT}: A new model of the global
propagation and dissipation of atmospheric gravity waves, Adv. Space Res., 20, 1253--1256,
1997.

\bibitem[{Ejiri et~al.(1999)Ejiri, Aso, Okada, Tsutsumi, Taguchi, Sato, and
Okano}]{Ejiri1999}
Ejiri, M., Aso, T., Okada, M., Tsutsumi, M., Taguchi, M., Sato, N., and Okano,
S.: Japanese research project on {Arctic} and {Antarctic} observations of the
middle atmosphere, Adv. Space Res., 24, 1689--1692, 1999.

\bibitem[{European Centre for Medium-Range Weather~Forecasts(1990)}]{cisl_rda_ds111.2}
European Centre for Medium-Range Weather~Forecasts.: {ECMWF TOGA 2.5 degree Global
Surface
and Upper Air Analyses},
\urlprefix\url{http://rda.ucar.edu/datasets/ds111.2/}, 1990. Accessed 30 April 2015

\bibitem[{Fairlie et~al.(1990)Fairlie, Fisher, and O'Neill}]{fairlie1990}
Fairlie, T., Fisher, M., and O'Neill, A.: The development of narrow baroclinic
zones and other small-scale structure in the stratosphere during simulated
major warmings, Q. J. R. Meteorol. Soc., 116,
287--315, 1990.

\bibitem[{Fritts and Alexander(2003)}]{fritts2003}
Fritts, D.~C. and Alexander, M.~J.: Gravity wave dynamics and effects in the
middle atmosphere, Rev. Geophys., 41, 2003.

\bibitem[{Garcia et~al.(1997)Garcia, Taylor, and Kelley}]{Garcia1997}
Garcia, F., Taylor, M.~J., and Kelley, M.: Two-dimensional spectral analysis of
mesospheric airglow image data, Appl. Opt., 36, 7374--7385, 1997.

\bibitem[{Gerrard et~al.(2002)Gerrard, Kane, Thayer, Duck,
Whiteway, and Fiedler}]{gerrard2002synoptic}
Gerrard, A.~J., T.~J. Kane, J.~P. Thayer, T.~J. Duck, J.~A. Whiteway, and
J.~Fiedler (2002), Synoptic scale study of the arctic polar vortex's
influence on the middle atmosphere, 1, observations, J. Geophys.
Res., 107(D16), ACL--1.

\bibitem[{Gerrard et~al.(2004)Gerrard, Kane, Eckermann, and
Thayer}]{gerrard2004}
Gerrard, A.~J., Kane, T.~J., Eckermann, S.~D., and Thayer, J.~P.: Gravity waves
and mesospheric clouds in the summer middle atmosphere: A comparison of lidar
measurements and ray modeling of gravity waves over Sondrestrom, Greenland,
J. Geophys. Res., 109, 2004.

\bibitem[{Gerrard et~al.(2011)Gerrard, Bhattacharya, and Thayer}]{gerrard2011}
Gerrard, A.~J., Bhattacharya, Y., and Thayer, J.: Observations of in-situ
generated gravity waves during a stratospheric temperature enhancement {(STE)}
event, Atmos. Chem. Phys., 11, 11\,913--11\,917, 2011.

\bibitem[{Guest et~al.(2000)Guest, Reeder, Marks, and Karoly}]{guest2000}
Guest, F.~M., Reeder, M.~J., Marks, C.~J., and Karoly, D.~J.: {Inertia-gravity
waves observed in the lower stratosphere over Macquarie Island}, J. Atmos. Sci., 57, 737--752,
2000.

\bibitem[{Hedin et~al.(1996)Hedin, Fleming, Manson, Schmidlin, Avery, Clark,
Franke, Fraser, Tsuda, Vial et~al.}]{hedin1996}
Hedin, A.~E., Fleming, E., Manson, A., Schmidlin, F., Avery, S., Clark, R.,
Franke, S., Fraser, G., Tsuda, T., Vial, F., et~al.: Empirical wind model for
the upper, middle and lower atmosphere, J. Atmos. Terr. Phys., 58, 1421--1447, 1996.

\bibitem[{Holton(1982)}]{holton1982}
Holton, J.~R.: The role of gravity wave induced drag and diffusion in the
momentum budget of the mesosphere, J. Atmos. Sci., 39,
791--799, 1982.

\bibitem[{Kaifler et~al.(2015)Kaifler, L{\"u}bken, H{\"o}ffner, Morris, and
Viehl}]{kaifler2015}
Kaifler, B., L{\"u}bken, F.-J., H{\"o}ffner, J., Morris, R.~J., and Viehl, T.~P., Lidar
observations of gravity
wave activity in the middle atmosphere over Davis (69$\degree$S, 78$\degree$E), Antarctica, J.
Geophys. Res.,
120(10), 4506-4521.

\bibitem[{Lane et~al.(2004)Lane, Doyle, Plougonven, Shapiro, and
Sharman}]{lane2004}
Lane, T.~P., Doyle, J.~D., Plougonven, R., Shapiro, M.~A., and Sharman, R.~D.:
Observations and numerical simulations of inertia-gravity waves and shearing
instabilities in the vicinity of a jet stream, J. Atmos. Sci., 61, 2692--2706, 2004.

\bibitem[{Li et~al.(2011)Li, Naqvi, Gerrard, Chau, and Bhattacharya}]{li2011}
Li, Z., Naqvi, S., Gerrard, A., Chau, J., and Bhattacharya, Y.: Numerical
modeling of lower stratospheric Doppler ducted gravity waves over Jicamarca,
Peru, Atmos. Chem. Phys., 11, 19\,011--19\,027,
2011.

\bibitem[{Lighthill(1978)}]{lighthill1978}
Lighthill, J.: Waves in Fluids, 504 pp, Cambridge Univ. Press, New York, 1978.

\bibitem[{Lin and Zhang(2008)}]{lin2008}

Lin, Y. and Zhang, F.: Tracking gravity waves in baroclinic jet-front systems, J. Atmos. Sci., 65, 2402--2415, 2008.

\bibitem[{Marks and Eckermann(1995)}]{marks1995}
Marks, C.~J. and Eckermann, S.~D.: A three-dimensional nonhydrostatic ray-tracing model for gravity waves: Formulation and preliminary results for the middle atmosphere, J. Atmos. Sci., 52, 1959--1984, 1995.

\bibitem[{Meriwether and Gerrard(2004)}]{meriwether2004}
Meriwether, J.~W. and Gerrard, A.~J.: Mesosphere inversion layers and stratosphere temperature enhancements, Rev. Geophys., 42, 2004.

\bibitem[{Moffat-Griffin et~al.(2011)Moffat-Griffin, Hibbins, Jarvis, and Colwell}]{moffat2011}
Moffat-Griffin, T., Hibbins, R.~E., Jarvis, M.~J., and Colwell, S.~R.: Seasonal variations of gravity wave activity in the lower stratosphere over an Antarctic Peninsula station, J. Geophys. Res., 116, 2011.

\bibitem[{Nielsen et~al.(2012)Nielsen, Taylor, Hibbins, Jarvis, and Russell}]{nielsen2012}
Nielsen, K., Taylor, M.~J., Hibbins, R., Jarvis, M., and Russell, J.: On the nature of short-period mesospheric gravity wave propagation over Halley, Antarctica, J. Geophys. Res., 117, 2012.

\bibitem[{O'sullivan and Dunkerton(1995)}]{o'sullivan1995}
O'sullivan, D. and Dunkerton, T.~J.: Generation of inertia-gravity waves in a simulated life cycle of baroclinic instability, J. Atmos. Sci., 52, 3695--3716, 1995.

\bibitem[{Oyama and Watkins(2012)}]{oyama2012}
Oyama, S. and Watkins, B.: Generation of atmospheric gravity waves in the polar thermosphere in response to auroral activity, Space Sci. Rev., 168, 463--473, 2012.

\bibitem[{Picone et~al.(2002)Picone, Hedin, Drob, and Aikin}]{picone2002}
Picone, J., Hedin, A., Drob, D.~P., and Aikin, A.: NRLMSISE-00 empirical model of the atmosphere: Statistical comparisons and scientific issues, J. Geophys. Res., 107, 2002.

\bibitem[{Plougonven et~al.(2003)Plougonven, Teitelbaum, and Zeitlin}]{plougonven2003}
Plougonven, R., Teitelbaum, H., and Zeitlin, V.: Inertia gravity wave generation by the tropospheric midlatitude jet as given by the Fronts and Atlantic Storm-Track Experiment radio soundings, J. Geophys. Res., 108, 2003.

\bibitem[{Plougonven and Snyder(2007)}]{plougonven2007}

Plougonven, R., and Snyder, C.: Inertia-gravity waves spontaneously generated by
jets and fronts. Part I: Different baroclinic life cycles, J. Atmos. Sci., 64, 2502--2520, 2007.

\bibitem[{Sato and Yoshiki(2008)}]{sato2008}
Sato, K. and Yoshiki, M.: Gravity wave generation around the polar vortex in
the stratosphere revealed by 3-hourly radiosonde observations at Syowa
Station, J. Atmos. Sci., 65, 3719--3735, 2008.

\bibitem[{Suzuki et~al.(2011)Suzuki, Tsutsumi, Palo, Ebihara, Taguchi, and
Ejiri}]{suzuki2011}
Suzuki, S., Tsutsumi, M., Palo, S., Ebihara, Y., Taguchi, M., and Ejiri, M.:
Short-period gravity waves and ripples in the South Pole mesosphere, J. Geophys. Res., 116,
2011.

\bibitem[{Tanaka and Tokinaga(2002)}]{tanaka2002}
Tanaka, H. and Tokinaga, H.: Baroclinic instability in high latitudes induced
by polar vortex: A connection to the Arctic Oscillation, J. Atmos. Sci., 59, 69--82, 2002.

\bibitem[{Vadas et~al.(2009)Vadas, Taylor, Pautet, Stamus, Fritts, Liu,
Sao~Sabbas, Rampinelli, Batista, and Takahashi}]{Vadas2009}
Vadas, S., Taylor, M., Pautet, P.-D., Stamus, P., Fritts, D., Liu, H.-L.,
Sao~Sabbas, F., Rampinelli, V., Batista, P., and Takahashi, H.: Convection:
the likely source of the medium-scale gravity waves observed in the OH
airglow layer near Brasilia, Brazil, during the SpreadFEx campaign, in:
Ann. Geophys., vol.~27, pp. 231--259, Copernicus GmbH, 2009.

\bibitem[{Wang and Alexander(2009)}]{wang2009}
Wang, L. and Alexander, M.~J.: Gravity wave activity during stratospheric
sudden warmings in the 2007--2008 Northern Hemisphere winter, J. Geophys. Res., 114, 2009.

\bibitem[{Whiteway and Duck(1999)}]{whiteway1999}
Whiteway, J.~A. and Duck, T.~J.: Enhanced Arctic stratospheric gravity wave
activity above a tropospheric jet, Geophys. Res. Lett., 26, 2453--2456, 1999.

\bibitem[{Yamashita et~al.(2010)Yamashita, Liu, and Chu}]{yamashita2010}
Yamashita, C., Liu, H.-L., and Chu, X.: Responses of mesosphere and lower
thermosphere temperatures to gravity wave forcing during stratospheric sudden
warming, Geophys. Res. Lett., 37, 2010.

\bibitem[{Yamashita et~al.(2013)Yamashita, England, Immel, and
Chang}]{yamashita2013}
Yamashita, C., England, S.~L., Immel, T.~J., and Chang, L.~C.: Gravity wave
variations during elevated stratopause events using SABER observations,
J. Geophys. Res., 118, 5287--5303, 2013.

\end{thebibliography}

%% FIGURES
%% ONE-COLUMN FIGURES
\newpage

\begin{figure}[t]
\includegraphics[width=12cm]{Figure-1.pdf}
\caption{Processed Na image from August 6, 2004. The images were unwarped onto a 400 x 400 km geographic grid (shown in the bottom left image) with the positive y-axis corresponding to 0$\degree$ longitude. Yellow circles mark the location of the observed wave in each image. Time stamps are shown in the bottom left of each image, and is read as YYYYMMDDHHMMSS. The sequence of images starts at the top left, and follows to the top right, bottom left, and finally bottom right.}
\label{Aug06Wave}
\end{figure}

\clearpage

\begin{figure}[t]
\includegraphics[width=12cm]{Figure-2.pdf}
\caption{Processed Na image from August 18, 2004. The images were unwarped onto a 400 x 400 km geographic grid (shown in the bottom left image) with the positive y-axis corresponding to 0$\degree$ longitude. Yellow circles mark the location of the observed wave in each image. Time stamps are shown in the bottom left of each image, and is read as YYYYMMDDHHMMSS. The sequence of images starts at the top left, and follows to the top right, bottom left, and finally bottom right.}
\label{Aug18Wave}
\end{figure}

\clearpage

\begin{figure}[t]
\includegraphics[width=12cm]{Figure-3.pdf}
\caption{(left) Results of the GROGRAT ``climatological'' run for the wave observed on August 06, 2004 using background pressures, temperatures, and horizontal winds reconstructed from NRLMSISE-00 and HWM-93. (right) Results of the GROGRAT run for the same wave using an atmosphere constructed from ECMWF Reanalysis below 50 km altitude and NRLMSISE-00 and HWM-93 between 50 km and 100 km altitude. The two contours in each panel represent

geopotential heights at 3 mbar (blue) and 10 mbar (green), and the red line in each panel
represents the wave ray path.}
\label{040806Runs}
\end{figure}

\clearpage

\begin{figure}[t]
\includegraphics[width=12cm]{Figure-4.pdf}
\caption{(left) Results of the GROGRAT "climatological" run for the wave observed on August
18, 2004 using background pressures, temperatures, and horizontal winds reconstructed from
NRLMSISE-00 and HWM-93. (right) Results of the GROGRAT run for the same wave using an
atmosphere constructed from ECMWF Reanalysis below 50 km altitude and NRLMSISE-00 and
HWM-93 between 50 km and 100 km altitude. The two contours in each panel represent
geopotential heights at 3 mbar (blue) and 10 mbar (green), and the red line in each panel
represents the wave ray path.}
\label{040819Runs}
\end{figure}

\clearpage

\begin{figure}[t]
\includegraphics[width=12cm]{Figure-5.pdf}
\caption{GROGRAT ray-tracing results for the August 19, 2004 wave shown in Figure 4 (right)
projected in 3-D over Antarctica. The two contours represent geopotential heights at 3 mbar
(blue) and 10 mbar (green), and show the wave ray path (red line).}
\label{Aug19Foregrats3d}
\end{figure}

\clearpage

\begin{figure}[t]
\includegraphics[width=12cm]{Figure-6.pdf}
\caption{Plots comparing horizontal wavelength(top left), period(top right), and phase speed
(bottom left) of the observed waves to the height of their sources as determined by individual
GROGRAT runs for the 87 wave events found to be freely propagating waves. The waves are
differentiated by month and year, with blue circles representing waves observed during June
2003, red 'x' marks denoting waves observed during August 2003, and green 'x' marks showing
waves observed during August 2004. The bottom right panel shows a plot of the latitude and
longitude of the wave sources near South Pole, from which it is apparent that all but 6 waves
originate within 2.5$\degree$ of SPA}
\label{PhaseSpeed}
\end{figure}

\clearpage

\begin{figure}[t]
\includegraphics[width=12cm]{Figure-7.pdf}
\caption{24-hr time differenced contour plots of geopotential height (black contours) and temperatures obtained from ECMWF Reanalysis from 0-50 km along the direction of the ray path for waves observed on July 18, 2003 (top left), July 22, 2003 (top right), August 2, 2003 (bottom left) and August 18, 2004 (bottom right), as determined by our GROGRAT model runs. Ticks on contour lines point to lower geopotential height. Vertical red lines mark the latitude at which the rays terminate, and the corresponding red 'X' denotes the location of the wave source. The yellow oval signifies the region where we infer baroclinic instability.}
\label{StratWaves}
\end{figure}

\clearpage

\begin{figure}[t]
\includegraphics[width=12cm]{Figure-8.pdf}
\caption{24-hr time differenced contour plots of geopotential height (black contours) and temperatures obtained from ECMWF Reanalysis from 0-50 km along the direction of the ray path for waves observed on July 19, 2003 (top left), August 3, 2003 (top right), August 17, 2003 (bottom left) and August 9, 2004 (bottom right), as determined by our GROGRAT model runs. Ticks on contour lines point to lower geopotential height. Vertical red line marks the latitude at which the ray terminates, and the corresponding red 'X' denotes the location of the wave source.}
\label{TropoWaves}
\end{figure}

\clearpage

\begin{figure}[t]
\includegraphics[width=12cm]{Figure-9.pdf}
\caption{24-hr time differenced contour plots of geopotential height (black contours) and temperatures obtained from ECMWF Reanalysis from 0-50 km along the direction of the ray path of the August 6, 2004 (left) and August 7, 2004 (right) waves, as determined by GROGRAT. Ticks on contour lines point to lower geopotential height.}
\label{MesoWaves}
\end{figure}

\end{document}